Application of a Perfectly Matched Layer to the Nonlinear Wave Equation

Daniel Appelö [*,1]

Center for Applied and Scientific Computing,
Lawrence Livermore National Laboratory, Livermore, Ca 94551, USA

Gunilla Kreiss [2]

Department of Information Technology, Division of Scientific Computing, Uppsala University, Uppsala S-75105, Sweden

---

Abstract

We derive a perfectly matched layer-like damping layer for the nonlinear wave equation. In the layer only two auxiliary variables are needed. In the linear case the layer is perfectly matched, but in the nonlinear case it is not. Well-posedness is established for the linear case. We also prove various energy estimates which can be used as a starting point for establishing stability of more general cases. In particular, we are able to show estimates for a special type of nonlinearity.

Numerical experiments that show the effectiveness of the layer are presented both for nonlinear and linear problems. In the computations we use an eighth order summation-by-parts discretization in space and implement the boundary conditions using a penalty procedure. We present new stability results for this discretization applied to the second order wave equation in the case with Dirichlet boundary conditions.

Key words: Perfectly matched layer, PML, Absorbing layers, Nonlinear waves
PACS: 05.45, 02.60

---

* Corresponding author: appelo2@llnl.gov
1 Supported, in part, by the Swedish research council grant no. VR2004-2371, Stiftelsen Lars Hiertas minne
2 Supported, in part, by the Swedish research council grant no. VR2004-2371

1 Introduction

Many wave propagation problems are formulated on domains with artificial boundaries, where boundary conditions must be formulated. Ideally the boundary conditions should yield a well posed problem, waves should pass without reflections and they should be easy to implement in a stable and accurate way. The perfectly matched layer (PML) technique is an example of such a boundary condition which has successfully been applied to many problems, as for example Maxwell's equations, the linear wave equation, Euler's equations linearized around various flows and the elastic wave equation (see further [8,2]). However, so far there are only a few nonlinear applications. In [14] a successful construction of a PML for the Euler equations is presented. Also, in some cases instabilities have been reported from nonlinear applications, see [1].

For time-dependent linear problems high order non-reflecting boundary conditions (NRBC) is an alternative to PML. Recently Givoli and Neta, [7] and Hagstrom and Warburton [11] have presented new formulations of Higdons, [12] classic boundary conditions, that fully exploit the asymptotics of the original formulation.

For the linear dispersive wave equation Givoli, Neta and Patlashenko, [6] have suggested corresponding high order NRBCs.

As for the PML technique there are only a few applications of NRBCs to nonlinear problems. One example is the recent paper by Szeftel, [24]. In [24] a family of absorbing boundary conditions for the semi-linear wave equation are developed via paradifferential calculus. Although the derivation of the boundary conditions are rather technical and only the first low order conditions are established, [24] is a contribution towards high order NRBCs for nonlinear wave equations.

In the present paper we study how the PML technique can be applied to the nonlinear dispersive wave equation. The mathematical properties of the nonlinear wave equation has been studied in numerous works (see any of the textbooks [23,16,13] for summary and references) and the mathematical theory treating singularities, local and global existence, solitons and inverse scattering is by now well developed. On the other hand, the development of numerical methods for the nonlinear wave equation have received much less attention, at least compared to numerical methods for conservation laws with discontinuous solutions. This lack of interest in the numerical analysis community for the nonlinear wave equation probably stems from the sparsity of applications it has been assumed to model. However, recently it was suggested, [21,22] that the nonlinear Klein-Gordon and related nonlinear wave equations can be used to model ratchet, or rectification, phenomena in nonlinear non- equilibrium systems, appearing in many fields like nanoscale devices, optical lattices [18], and molecular biology, [19]. The study of such phenomena motivates the developments of new numerical techniques for the nonlinear wave equation.

Our approach to construct a PML for the nonlinear wave equation is straightforward. We simply construct a PML for the linearized equation, and then apply it to the corresponding nonlinear equation. We use the modal ansatz construction which was introduced by Hagstrom, [9], for first order systems. In this paper we use the same type of ansatz but construct a layer directly for the second order formulation of the wave equation. Although the nonlinear absorbing layer is not perfectly matched, for convenience, we will refer to it as the nonlinear PML or simply PML.

For the linear equation the construction we use guarantees perfect matching. Well-posedness and stability is however not guaranteed. One way to investigate these properties is to consider the linear, constant coefficient problem. After Fourier transform in the spatial directions, determining well-posedness and stability is an algebraic problem, see [17]. In [10] techniques were developed to automatically determine Petrowskii well-posedness and stability of constant coefficient Cauchy problems. These techniques were applied to various PML models in [3]. Although the techniques in [10] are automatic and generate energy estimates for constant coefficient problems, results derived in this way are rather difficult to extend to variable coefficient cases and to nonlinear cases. The difficulty is due to the high order of the derivatives appearing in the energy estimates.

Here, we will instead derive energy estimates by classical techniques using integration by parts. With these techniques it is harder to come up with a suitable energy candidate (in general, one has to make an educated guess). However, once an energy is found, it is often more compact and thus the extension to variable coefficients may be less difficult. For Bérenger's PML for Maxwells equations in two dimensions Bécache and Joly, [4], derived various energy estimates. Since Maxwells equations in two dimensions can be reduced to the wave equation we expect the linear versions of our estimates to have similarities with the estimates in [4]. However, since we use a different PML, and include dispersive and nonlinear terms it is not surprising that the estimates are not identical.

For the dispersive wave equation there is a well known energy estimate that holds in the computational domain, outside the PML. Inside the PML we derive a related estimate. The estimate is valid for constant damping coefficients and for certain nonlinear terms. We also present an energy estimate for the non-dispersive wave equation with variable damping coefficient.

We also present computations showing the efficiency of the suggested nonlinear PML for various nonlinearities. To be able to estimate the efficiency of our PML we have implemented a nonlinear version of the standard absorbing layer without the perfect matching property suggested by Israeli and Orzag, [15]. For the linear dispersive case we compare our results to existing high order non-reflecting boundary conditions, see [6]. Since the numerical examples of [24] are restricted to one dimension we have not been able to compare its performance relative our PML.

To obtain an accurate solution we discretize the equations with high order finite difference approximations with the summation-by-parts property and implement the boundary conditions using a penalty procedure, see [5]. We also present new stability results for this discretization applied to the second order wave equation in the case with homogenous Dirichlet boundary conditions.

2 The Wave Equation with Power Type Nonlinearities

We consider the nonlinear wave equation

$$\partial_t^2 u - \nabla^2 u = -f(u, \partial_t u), \tag{1}$$

in $n+1$ dimensions $(t, x, y_1, \dots, y_n)$, with power type nonlinearities. Specifically we take $f(u, \partial_t u)$

$$f(u, \partial_t u) = \sum_{k \geq 0} c_k u^{2k+1} + \sum_{k \geq 0} d_k \partial_t u^{2k+1}, \quad c_k \geq 0,\, d_k \geq 0. \tag{2}$$

The nonlinearity (2) includes, for example, the so called ϕ^4 equation that together with the Sine-Gordon equation has been suggested as models for ratchet dynamics appearing in many physical systems, see [21] and references within.

There is a very large body of literature that concerns the mathematical properties of (1). For example there are numerous different types of estimates and inequalities that can be used to investigate local and global existence of the Cauchy problem, see e.g. [16]. Here we will only make use of the most well known result, concerning the following energy estimate for the Cauchy problem or for problems on bounded domains with homogenous Dirichlet or Neuman boundary

$$\begin{aligned}\frac{d}{dt}\left(\|\partial_t u\|^2 + \|\partial_x u\|^2 + \sum_{l=1}^{n} \|\partial_{y_l} u\|^2 + \sum_{k\geq 0} \frac{c_k}{2k+2}\|u^{k+1}\|^2\right) = \\ = -\sum_{k \geq 0} d_k \|\partial_t u^{k+1}\|^2.\end{aligned} \tag{3}$$

Here and for the remainder of this paper $\|\cdot\|$ denotes the L_2 norm. We will denote the corresponding inner product by $(\cdot,\cdot)$.

3 A PML-like Absorbing Layer for the Nonlinear Wave Equation: Second Order Formulation

To derive a PML-like absorbing layer for the equation (1) we first construct the PML for the linear problem obtained by the specific right hand side $f(u) = c_0 u$. To construct a PML for a second order equation we use the techniques introduced by Hagstrom, [9], for first order systems. The construction can be summarized by the following steps

(1) Perform a Laplace transform in time and a Fourier transfor in the tangential directions of the governing equations.
(2) Make a modal ansatz with spatially exponentially decaying amplitude in the propagating direction.
(3) Construct equations in the layer supporting the ansatz, and satisfying a compatability condition: continuity across the interface should imply continuity of derivatives across the interface (this will ensure the perfect matching).
(4) Localize in time by introducing auxiliary functions.
(5) Invert the transforms.

For a layer in the strip $0 < x < L$ we perform a Laplace transform in time and a Fourier transform in the tangential directions

$$\left[s^2 + (|k_y|^2 + c_0)\right]\hat{u} = \frac{d^2\hat{u}}{dx^2}. \tag{4}$$

Here $|k_y|^2 = k_{y_1}^2 + k_{y_2}^2 + \dots$ is the sum of the squares of the duals in the tangential directions, s is the Laplace transform dual.

Inserting modal solutions $\hat{u} = \hat{\phi}e^{\lambda x}$ into (4) we obtain the eigenvalue problem

$$\left[-s^2 + \lambda^2 - (|k_y|^2 + c_0)\right]\hat{\phi} = 0. \tag{5}$$

In the layer we postulate the modal solution

$$\hat{u} = \hat{\phi}e^{\lambda x + \frac{\lambda}{s+\alpha}\int_0^x \sigma(z)dz}. \tag{6}$$

Taking d/dx of (6) we get

$$\lambda\hat{u} = \left(1 - \frac{\sigma(x)}{s+\alpha+\sigma}\right)\frac{d}{dx}\hat{u} = (\frac{s+\alpha}{s+\alpha+\sigma(x)})\frac{d}{dx}\hat{u}. \tag{7}$$

To construct the layer equations, supporting the modal ansatz (6) with λ determined by (5), we replace $\frac{d}{dx}$ with $(\frac{s+\alpha}{s+\alpha+\sigma(x)})\frac{d}{dx}$ in (4) and obtain

$$\left[-s^2 + (\frac{s+\alpha}{s+\alpha+\sigma(x)})\frac{d}{dx}(1 - \frac{\sigma(x)}{s+\alpha+\sigma(x)})\frac{d}{dx} - (|k_y|^2 + c_0)\right]\hat{u} = 0. \quad (8)$$

By inserting $\hat{u} = \hat{\varphi}e^{\kappa(x)}$ into (8) it can be verified that the solution is of the postulated form (6). Also note that the compatibility condition is satisfied if $\sigma(0) = 0$.

We can rewrite (8) as

$$\left[s^2\frac{s+\alpha+\sigma(x)}{s+\alpha} - \frac{d}{dx}(1 - \frac{\sigma(x)}{s+\alpha+\sigma(x)})\frac{d}{dx} + (|k_y|^2 + c_0)(1 + \frac{\sigma(x)}{s+\alpha})\right]\hat{u} = 0.$$

To localize in time we introduce the auxiliary variable

$$\hat{\eta}^{(1)} = -\frac{1}{s+\alpha+\sigma(x)}\frac{d\hat{u}}{dx}.$$

This gives us

$$s^2\frac{s+\alpha+\sigma(x)}{s+\alpha}\hat{u} = \frac{d}{dx}(\frac{d}{dx}\hat{u} + \sigma(x)\hat{\eta}^{(1)}) - (|k_y|^2 + c_0)\hat{u} - \frac{\sigma(x)(|k_y|^2 + c_0)}{s+\alpha}\hat{u}.$$

Now we use the identity $s^2 = (s+\alpha)(s-\alpha) + \alpha^2$, and get

$$\begin{aligned}
((s+\alpha)(s-\alpha) + \alpha^2)\frac{s+\alpha+\sigma(x)}{s+\alpha}\hat{u} &= \\
(s-\alpha)(s+\alpha+\sigma(x))\hat{u} + \left(\alpha^2 + \alpha^2\frac{\sigma(x)}{s+\alpha}\right)\hat{u} &= \\
s(s+\sigma(x))\hat{u} - \alpha\sigma(x)\left(1 - \frac{\alpha}{s+\alpha}\right)\hat{u} &= \\
+\frac{d}{dx}(\frac{d}{dx}\hat{u} + \sigma(x)\hat{\eta}^{(1)}) - (|k_y|^2 + c_0)\hat{u} - \frac{\sigma(x)(|k_y|^2 + c_0)}{s+\alpha}\hat{u}.
\end{aligned}$$

By finally introducing

$$\hat{\eta}^{(2)} = \frac{-\alpha^2 - |k_y|^2 - c_0}{s+\alpha}\hat{u},$$

we can invert the transforms. We obtain the following set of equations in the layer

$$\begin{aligned}
&\partial_t^2 u - \nabla^2 u = -\sigma(x)\partial_t u + \sigma(x)\eta^{(2)} + \alpha\sigma(x)u - c_0 u + \partial_x\left(\sigma(x)\eta^{(1)}\right), \\
&\partial_t\eta^{(1)} + (\sigma(x) + \alpha)\eta^{(1)} + \partial_x u = 0, \\
&\partial_t\eta^{(2)} + \alpha\eta^{(2)} = \nabla_y^2 u - (c_0 + \alpha^2)u.
\end{aligned} \quad (9)$$

Here $\nabla_y^2 w = (\sum_{l=1}^n \partial_{y_l}^2)w$. The corresponding PML for the nonlinear problem is

$$\partial_t^2 u - \nabla^2 u = -\sigma(x)\partial_t u + \sigma(x)\eta^{(2)}$$
$$+\alpha\sigma(x)u + f(u, \partial_t u) + \partial_x \left(\sigma(x)\eta^{(1)}\right), \tag{10}$$
$$\partial_t \eta^{(1)} + (\sigma(x) + \alpha)\eta^{(1)} + \partial_x u = 0, \tag{11}$$
$$\partial_t \eta^{(2)} + \alpha\eta^{(2)} = \nabla_y^2 u - \alpha^2 u + f(u, \partial_t u). \tag{12}$$

The well-posedness of the linear system (9) can be established by considering a corresponding first order system obtained by introducing $i|k|\hat{w} = \hat{u}_t$. Since the PML is a lower order perturbation of the original problem an appropriate boundary condition terminating the layer is either a Dirichlet or a Neumann condition. Note also that no boundary conditions should be imposed on $\eta^{(1)}$. This can be seen by analyzing the number of nonzero eigenvalues of the symbol of the first order system. For this system the $\partial_x \eta^{(1)}$ term will correspond to the zero order term $ik_x/|k|\hat{\eta}^{(1)}$.

4 Energy Estimates

In this section we consider energy estimates and the stability of the Cauchy problem for the PML. Here the term energy estimates does not refer to a physical energy but rather to bounds in time on the L_2-norm of functions or derivatives of them, see [17]. For simplicity of notation we will in this section assume variations in only two space dimensions, x and y. The generalization to more space dimensions is straightforward. In the linear case, with constant $\sigma \geq 0$, $\alpha \geq 0$, the characteristic equation, or dispersion relation of equation (9) is obtained by inserting plane wave solutions (note that λ is not the same as in the previous section)

$$u = Ue^{\lambda t + i(k_x x + k_y y)}. \tag{13}$$

The dispersion relation then becomes

$$\lambda^2(\lambda + \alpha + \sigma)^2 + k_x^2(\lambda + \alpha)^2 + (k_y^2 + c_0)(\lambda + \alpha + \sigma)^2 = 0. \tag{14}$$

In [3], Section 4, stability of a PML for Maxwell's equation is investigated. That system has the dispersion relation

$$\lambda(\lambda^2(\lambda + \alpha + \sigma)^2 + k_x^2(\lambda + \alpha)^2 + k_y^2(\lambda + \alpha + \sigma)^2) = 0. \tag{15}$$

We note that with $\tilde{k}_y = \sqrt{k_y^2 + c_0}$ our dispersion relation, (14), multiplied with λ gives (15). A, for our purposes, relevant result in [3] is that all roots of (15) have non-positive real parts. This proves that all roots of $\lambda(k_x, k_y)$ of (14) have non-positive real parts, implying stability for the linear, constant coefficient case. Also several energies are given. For example, there is a decaying energy involving high derivatives, but also a simpler energy that is only guaranteed to be bounded. This energy is easily extended to $c_0 > 0$ implying

$$(\alpha + \sigma)^2 \left(\|\partial_x \partial_y u\|^2 + c_0 \|\partial_x u\|^2 \right) + \alpha^2 \|\partial_x^2 u\|^2 \leq C_0.$$

Here C_0 is a constant depending only on the initial data.

To obtain more general stability results, for variable $\sigma(x)$ and in the presence of nonlinear terms, energy estimates are needed. We can derive estimates directly from the equation, using only integration by parts. To begin with we note that in the linear case, the dispersion relation corresponding to (1) is

$$\lambda^2 + k_x^2 + k_y^2 + c_0 = 0,$$

and by (3)

$$\|\partial_t u\|^2 + \|\partial_x u\|^2 + \|\partial_y u\|^2$$

is bounded. The resemblance between this dispersion relation and (14) suggests that we try to derive an estimate for

$$E(t) = \|\partial_t^2 u + (\sigma + \alpha)\partial_t u\|^2 + \|\partial_x \partial_t u + \alpha \partial_x u\|^2 + \|\partial_x \partial_t u + (\sigma + \alpha)\partial_y u\|^2.$$

The proofs of the results given below can be found in Appendix A.1.

Theorem 1. *Consider the Cauchy problem for the system (10-12) with σ and α constant. All solutions satisfy*

$$\begin{aligned}
&\|\partial_t^2 u + (\sigma + \alpha)\partial_t u\|^2 + \|\partial_t \partial_y u + (\sigma + \alpha)\partial_y u\|^2 + \\
&\quad + \|\partial_x \partial_t u + \alpha \partial_x u + \sigma(\partial_t \eta^{(1)} + \alpha \eta^{(1)})\|^2 + \\
&\quad + 2\sigma\alpha \|\partial_t \eta^{(1)} + \alpha \eta^{(1)}\|^2 + \|\sigma \partial_t \eta^{(1)}\|^2 + \|\sigma \alpha \eta^{(1)}\|^2 = \\
&\quad = C_0 - 2 \int_0^t (\sigma \|\partial_t \eta^{(1)} + \alpha \eta^{(1)}\|^2 + \alpha \|\sigma \partial_t \eta^{(1)}\|^2 + \mathcal{F}) d\tau.
\end{aligned}$$

Here C_0 is given by the initial data, and

$$\mathcal{F} = \left(\partial_t^2 u + (\sigma + \alpha)\partial_t u, \partial_t f(u, \partial_t u) + (\sigma + \alpha) f(u, \partial_t u) \right). \tag{16}$$

Remark 2. With variable $\sigma(x)$ an extra term in $\frac{d}{dt}E(t)$ appears,

$$I_4 = \left(\frac{d\sigma}{dx} \partial_t u, (\partial_t + \alpha)^2 \eta^{(1)} \right). \tag{17}$$

If this term could be estimated in terms of the other quantities appearing in the theorem we would have a useful estimate for the variable coefficient case. We have not been able to derive such an estimate.

For the nonlinear term we have only been able to derive useful expressions for special cases. We have

Lemma 3. *Consider the nonlinear term* $\mathcal{F}$ *with* $f(u, \partial_t u) = c_0 u + d_p \partial_t u^{2p+1}$, *where* p *is a positive integer. Then*

$$\mathcal{F} = \frac{1}{2}\frac{d}{dt}\left(c_0\|\partial_t u + (\sigma+\alpha)u\|^2 + 4pd_p(\sigma+\alpha)\|\partial_t u^{p+1}\|^2\right) + \tag{18}$$

$$d_p\|\partial_t u^p(\partial_t^2 u + (\sigma+\alpha)\partial_t u)\|^2 + 2pd_p\|\partial_t^2 u \partial_t u^p\|^2. \tag{19}$$

In the linear case,

$$f(u) = cu, \quad c \geq 0, \tag{20}$$

we can for the case, $\alpha = 0$, derive another bound. The proof follows the same lines as in the other cases, and can be found in the appendix.

Theorem 4. *With* $\alpha = 0$, *constant* $\sigma > 0$, *and (20) all solutions of the Cauchy problem for (10-12) satisfy*

$$\|\partial_t^2 u\|^2 + \|\partial_t\partial_y u\|^2 + \|\partial_t\partial_x u + \sigma\partial_t\eta^{(1)}\|^2 + \sigma\|\partial_y\eta^{(1)}\|^2 + \|\sigma\eta^{(2)}\|^2 + \\ + \|\sigma\partial_y u\|^2 + c\|\sigma u\|^2 + c\|\partial_t u\|^2 + c\|\sigma\eta^{(1)}\|^2 \leq C_0,$$

where C_0 *depends only on the initial data.*

For the special case $c = 0$ this estimate can be compared with the estimate in Theorem XYZ in [4]. We note that for $\sigma = 0$ and $c = 0$ this estimate reduces to the standard estimate (3) for the time derivative of the wave equation, while the estimate in [4] reduces to the the standard estimate.

5 High Order Discretization of the Wave Equation

In this section we will discuss high order approximations of the wave equation in one space dimension. We will present a new stability result for the discretization of the case with homogenous Dirichlet boundary conditions. In the next section the approximations will be extended to more space dimensions and to include dispersive and nonlinear terms.

The time integration will be performed by a 8th order 12 stage Runge-Kutta method [25].

For the approximation of spatial derivatives we will use finite difference operators with the summation-by-parts property (SBP operators, in short). The boundary conditions will be imposed by the simultaneous approximation technique, SAT (see, [5,20]). In [20] it has been shown how Neumann and Robin conditions for the wave equation can be imposed by the SAT technique. However, the case of homogenous Dirichlet boundary conditions was not discussed. Below we will show that this case can be handled as well.

The SBP+SAT technique is best described by a simple example (borrowed from [20]). Consider the 1D wave equation with mixed homogenous boundary conditions

$$\partial_t^2 u = \partial_x^2 u, \quad x \in [0,1]. \tag{21}$$

$$a_l u(t,0) + b_l \partial_x u(t,0) = 0,\ b_l \neq 0, \quad a_r u(t,1) + b_r \partial_x u(t,1) = 0,\ b_r \neq 0. \tag{22}$$

Using equation (21), integration by parts and the boundary conditions (22) it is easy to show that

$$\frac{d}{dt}\left(\|\partial_t u\|^2 + \|\partial_x u\|^2\right) = 2\partial_t u \partial_x u|_0^1 = -\frac{d}{dt}\left(\frac{a_r}{b_r}(\partial_t u(t,1))^2 - \frac{a_l}{b_l}(\partial_t u(t,0))^2\right).$$

Thus if

$$a_l/b_l < 0,\ a_r/b_r > 0 \tag{23}$$

there is an energy estimate.

To discretize (21) we introduce a equidistant grid with $N+1$ grid points, $x_i = i \cdot h$, $i = 0, \dots, N$ where $h = 1/N$. At each grid point we define a grid function $v_i(t)$ approximating $u(t, x_i)$. Also let $v = [v_0, \dots, v_N]^T$,$E_0 = \mathrm{diag}([1, 0, \dots, 0])$, $E_N = \mathrm{diag}([0, \dots, 0, 1])$ and $B = \mathrm{diag}([-1, 0, \dots, 0, 1])$.

Using the definitions from [20] we say that.

Definition 5. Let $D_2 = H^{-1}(-A + BS)$ be a difference operator approximating $\partial^2/\partial x^2$. It is called a second derivative SBP operator if the following conditions are met

$$\begin{aligned} &(1) \quad A + A^T \geq 0, \\ &(2)\ BSv = \begin{bmatrix} -D_{1+}v_0 \\ 0 \\ \vdots \\ 0 \\ D_{1-}v_N \end{bmatrix}. \end{aligned} \tag{24}$$

Here D_{1+} and D_{1-} are one-sided difference operators approximatint $\partial/\partial x$ and v is a gridfunction.

Using a SBP difference operator together with the SAT to enforce the boundary conditions results in the following semi-discrete approximation of (21-22)

$$
\begin{aligned}
&\partial_t^2 v = \tilde{D}_2 v, \\
&\tilde{D}_2 = D_2 + \tau_l H^{-1} E_0 (a_l I + b_l S) + \tau_r H^{-1} E_N (a_r I + b_r S).
\end{aligned}
\tag{25}
$$

If the penalty parameters are chosen as

$$
\tau_l = \frac{1}{b_l}, \quad \tau_r = -\frac{1}{b_r}, \tag{26}
$$

it has been shown (Lemma A.1, [20]) that, when (23) holds and D_2 is a symmetric second derivative SBP operator, (25) has non growing solutions. The proof relies on the fact that $\tilde{D}_2$ is a symmetric operator.

5.1 A Stability Result for Homogenous Dirichlet Boundary Conditions

One important case, the case of homogenous Dirichlet boundary conditions, is not included in Lemma A.1 in [20]. Then $a_l = a_r = 1$, $b_l = b_r = 0$ and

$$
\tilde{D}_2 = D_2 + \tau_l H^{-1} E_0 + \tau_r H^{-1} E_N, \tag{27}
$$

is non-symmetric. For this case we will prove stability for sufficiently large τ in a diagonal norm case.

To determine stability of (25) we need to consider the eigenvalues of $\tilde{D}_2$, or equivalently the eigenvalues of $M = C\tilde{D}C^T$. Here $\tilde{D} = H\tilde{D}_2$ and $H^{-1} = C^T C$ (the Cholesky factorization of the symmetric positive definite matrix H^{-1}). Note that in the case under consideration neither M nor $\tilde{D}$ are symmetric, and for general C the matrix M may not have real eigenvalues even if $\tilde{D}$ has real eigenvalues. Also note that in the diagonal norm case,

$$
H = \mathrm{diag}(h_0, h_1, \ldots, h_N), \quad C = C^T = \mathrm{diag}(h_0^{-1/2}, \ldots, h_N^{-1/2}).
$$

Introduce the following notation for the inner block of the matrix

$A = (A_{ij})$, $0 \le i, j \le N$,

$$\tilde{A} = \begin{pmatrix} A_{11} & \dots & A_{1,N-1} \\ \vdots & & \vdots \\ A_{N-1,1} & \dots & A_{N-1,N-1} \end{pmatrix}.$$

Theorem 6. *Consider (25) with $a_l = a_r = 1$ and $b_l = b_r = 0$. Assume H is diagonal, A symmetric and positive semi-definite and that CAC has inner block with distinct positive eigenvalues. There exist a $\tau_{\min} \gg 1$ such that if*

$$\tau_l = \tau_r \ge \tau_{\min}. \tag{28}$$

then (25) is stable. Here $C^2 = H^{-1}$.

Proof. We need to analyze the eigenvalues of

$$M = C\tilde{D}C = -CAC - CBSC - \frac{\tau_l}{h_0}E_0 - \frac{\tau_r}{h_N}E_N. \tag{29}$$

Note that $G = CAC$ is symmetric and positive semi-definite, and that $CBSC = BCSC$. If $\sigma_l = \tau_l/h_0$ and $\sigma_r = \tau_r/h_N$ are sufficiently large the theorem follows from the two lemmas below. □

Remark 7. The standard second order accurate SPB operator D_2 with diagonal norm satisfies the requirements of theorem 6.

The symmetric $G + \sigma_l E_0 + \sigma_r E_N$ has real eigenvalues. Lemma 8 states conditions that ensure that the eigenvalues are also distinct, and possible to approximate using Gershgorins theorem. In lemma 9, we need these results to prove that the eigenvalues of the non-symmetric M, eqn (29), are real and negative.

Lemma 8. *Assume G is symmetric and positive semi-definite, with inner block $\tilde{G}$ having distinct, positive eigenvalues μ_j. The matrix*

$$D = G + \sigma_l E_0 + \sigma_r E_N, \quad \sigma_l, \sigma_r \ge \sigma_{\min} > 0. \tag{30}$$

is also symmetric and positive semi-definite. If $\sigma_{\min}$ is sufficiently large the eigenvalues and eigenvectors of D are

$$\lambda_0 = \sigma_l + \mathcal{O}(1) > 0, \quad x_0 = e_0 + \mathcal{O}(\frac{1}{\sigma_{\min}}), \tag{31}$$

$$\lambda_j = \mu_j + \mathcal{O}(\frac{1}{\sigma_{\min}}) > 0, \quad x_j = \tilde{x}_j + \mathcal{O}(\frac{1}{\sigma_{\min}}),\ j = 1, \dots, N-1, \tag{32}$$

$$\lambda_N = \sigma_r + \mathcal{O}(1) > 0, \quad x_N = e_N + \mathcal{O}(\frac{1}{\sigma_{\min}}). \tag{33}$$

Here $e_0 = (1, 0, \dots, 0)^T$, $e_N = (0, \dots, 0, 1)^T$ *and* $\tilde{x}_j = (0, y_j^T, 0)^T$, *where* y_j *are the eigenvectors of the inner block* $\tilde{G}$.

Proof. Note that D is symmetric, and since E_0 and E_N are rank one matrices D is positive semi-definite. The first halves of (31) and (33) follow by Gerschgorin's theorem. The second halves of these statements follow by considering the power method with initial vectors e_0 and e_N, respectively. Next introduce an approximate diagonalizing transformation X_0

$$X_0 = (x_0, \tilde{x}_1, \dots \tilde{x}_{N-1}, x_N)\,.$$

Clearly X_0 is invertible and

$$X_0^{-1} = \mathrm{diag}(1, Y^{-1}, 1) + \mathcal{O}(\frac{1}{\sigma_{\min}}).$$

Thus

$$X_0^{-1} D X_0 = -\begin{pmatrix} \lambda_0 & \mathcal{O}(1) & 0 \\ 0 & Y^{-1}\tilde{A}Y + \mathcal{O}(\frac{1}{\sigma_{\min}}) & 0 \\ 0 & \mathcal{O}(1) & \lambda_N \end{pmatrix}.$$

The eigenvalues of this matrix are λ_0, λ_N and eigenvalues of the middle block, which (by Gerschgorin) are $\mu_j + \mathcal{O}(\frac{1}{\sigma_{\min}})$. For large $\sigma_{\min}$ these are distinct, and one can again apply some variant of the power method to show that the second half of (32) follows. □

Lemma 9. *Under the same assumptions as in the previous lemma there is a* $\sigma_{\min} \gg 1$ *such that*

$$\tilde{D} = -D - BCSC, \tag{34}$$

has real, negative eigenvalues.

Proof. By the previous lemma, if σ_{min} is sufficiently large, the symmetric matrix D has real, distinct, negative eigenvalues, and we know the diagonalizing matrix X consisting of the D's orthogonal eigenvectors. Apply the same diagonalizing transformation to $\tilde{D}$, yielding $X^T\tilde{D}X = \Lambda - X^T BCSCX$, where

$$X^T BCSCX = |\frac{s_{00}}{h_0}|E_0 + |\frac{s_{NN}}{h_N}|E_N + \mathcal{O}(\frac{1}{\sigma_{\min}}).$$

Here s_{ij} is a component of S and h_i is a diagonal element of H. If $\sigma_{\min}$ sufficiently large the off-diagonal perturbations caused by the non-symmetric terms are sufficiently small for the Gerschgorin discs to remain separate and in the negative half plane. Since complex eigenvalues only appear in conjugate pairs the eigenvalues must be real and negative. □

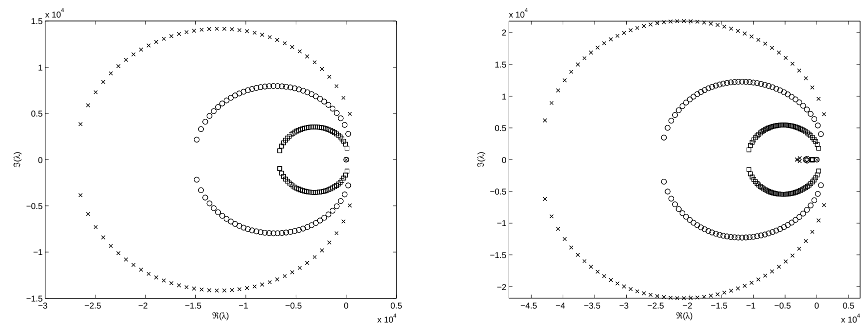

Fig. 1. To the left the spectrum of the full norm 6th order SBP, to the right the full norm 8th order. Only eigenvalues with nonzero imaginary part are plotted. The crosses are for $h = 2/100$, circles $h = 2/75$ and squares $h = 2/50$. For any of the curves increasing the value of γ moves the locations of the eigenvalues, starting close to the origin for small γ, along the circle arcs and back towards the real axis.

It remains to prove stability in more general cases. However, we have found, empirically, that for the full norm 6th and 8th order SBP operators, the discretization (27) with $\tau_l = \tau_r = -\gamma/h$ is stable and accuracy preserving, for suitably chosen γ. In Figure 1 the location of the eigenvalues with non-zero imaginary part of the matrix $\tilde{D}_2$ are plotted for different values of γ and h (see the caption for details). For the matrix $\tilde{D}_2$ we have numerically computed all eigenvalues for $h = 2/N, N = 20, 40, \ldots, 400$, for values of γ from 0 to 5 with steps of 0.05. For the 6th order full norm SBP operator we found that with $\gamma \geq 3.85$ all eigenvalues were real. The corresponding number for the eight order case was $\gamma \geq 4.50$. These numbers were independent of h.

5.2 Accuracy of the Discretization

We have also verified the order of accuracy by numerical experiments. In a first experiment we solve

$$\begin{aligned} \partial_t^2 u = \partial_x^2 u - \sin(t)(3541 + 3600x^2 - 7200x)\exp -30(x-1)^2), \quad x \in [0,2], \\ u(0,x) = 0,\ \partial_t u(0,x) = \exp\left(-30(x-1)^2\right),\ u(t,0) = u(t,2) = 0, \end{aligned} \tag{35}$$

which has the solution $u(t,x) = \sin(t)\exp\left(-30(x-1)^2\right)$. In the left subfigure in Figure 2 the convergence of the l_2 norm of the error at time 1 is plotted for the 6th and 8th order full norm SBPs (with $\gamma = 3.85$ and 4.50) and for the 2nd order diagonal norm SBP (with $\gamma = 4.50$). In the right subfigure the convergence of the l_2 norm of the error at time 2 is plotted for the problem

$$\begin{aligned} &\partial_t^2 u = \partial_x^2 u, \quad x \in [0,2], \\ &u(0,x) = \exp\left(-30(x-1)^2\right),\ \partial_t u(0,x) = 0,\ u(t,0) = u(t,2) = 0. \end{aligned} \tag{36}$$

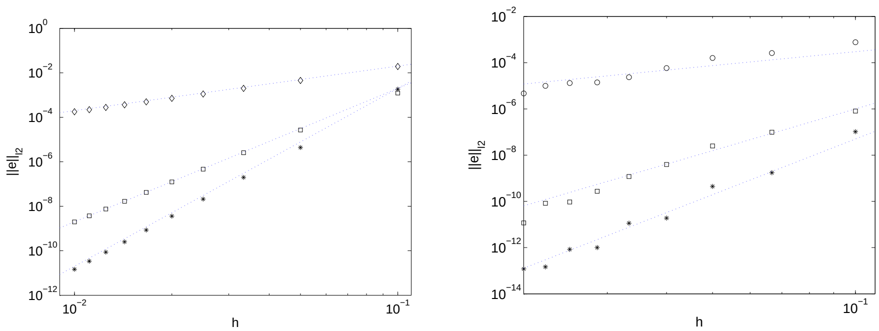

Fig. 2. The l_2 norm of the error for the problems (35) and (36). The diamond (left) and circle (right) are errors measured using the 2nd order diagonal norm, the squares using the 6th order full norm and the stars using the 8th order full norm. The dotted lines are proportional to h^2, h^6 and h^8.

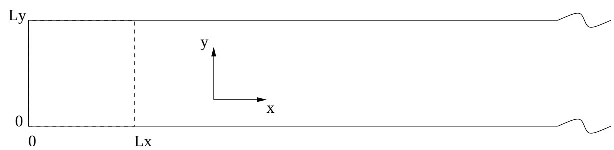

Fig. 3. Test problem setup

Note that the exact solution of (36), at time 2, coincides with the initial data. Again γ is chosen as suggested by the numerical study of the eigenvalues of $\tilde{D}_2$.

6 Numerical Experiments

In this section we present numerical results that show the effectiveness and stability of our PML in linear and nonlinear cases. For the nonlinear computations we will compare with a nonlinear version of the simple damping layer suggested by Israeli and Orzag, [15]. We will also compare our results for a linear dispersive problem with the results from [6], obtained with high order NRBCs.

In all of our experiments we will consider wave propagation in a two dimensional wave guide. The wave guide occupies the unbounded domain $(x, y) \in [0, \infty) \times [0, L_y]$ and the solution is to be computed in the bounded domain $(x, y) \in [0, L_x] \times [0, L_y]$, see Figure 3. The boundary conditions at $x = 0$, $y = 0$, $y = L_y$ are homogenous Dirichlet or Neumann boundary conditions and in the layer $L_x \leq x \leq L_x + L_{lay}$ we will use either our PML or the simpler damping layer suggested by Israeli and Orzag, [15]. The layers are terminated with a homogenous Dirichlet condition at $x = L_x + L_{lay}$.

Since we will use a high order method the damping function $\sigma(x)$ should be sufficiently smooth at the interface between the computational domain and the PML. Here we choose the damping functions to be

$$\sigma(x) = \begin{cases} \sigma_{max}(1 - (\frac{x-(L_x+L_{lay})}{L_{lay}})^2)^8 & L_x \leq x \leq L_x + L_{lay}, \\ 0 & \text{else.} \end{cases}$$

Here L_{lay} is the width of the layer and σ_{max} is the strength.

6.1 Discretization of the PML Equations

For simplicity we solve equations (10-12) both in the computational domain and in the layer. To do so we introduce an equidistant $N + 1 + N_l \times M + 1$ grid (N_l is the number of points in the layer)

$$x_i = ih_x, \qquad i = 0, 1, \ldots, N + N_l, \qquad h_x = \frac{L_x}{N}, \tag{37}$$

$$y_j = jh_y, \qquad j = 0, 1, \ldots, M, \qquad h_y = \frac{L_y}{M}. \tag{38}$$

Denote $u_{ij} = u(x_i, y_j)$, $\eta_{ij}^{(1)} = \eta^{(1)}(x_i, y_j)$, $\eta_{ij}^{(2)} = \eta^{(2)}(x_i, y_j)$ and let $v, \zeta^{(1)}$ and $\zeta^{(2)}$ be the three $(N + 1 + N_l)(M + 1) \times 1$ vectors approximating $u, \eta^{(1)}$ and $\eta^{(2)}$, i.e.

$$\begin{aligned} v^T \approx& [u_{11}, u_{12}, \ldots, u_{1M+1}, u_{21}, \ldots, u_{N+1+N_l\, M+1}], \\ (\zeta^{(1)})^T \approx& [\eta_{11}^{(1)}, \eta_{12}^{(1)}, \ldots, \eta_{1M+1}^{(1)}, \eta_{21}^{(1)}, \ldots, \eta_{N+1+N_l\, M+1}^{(1)}], \\ (\zeta^{(2)})^T \approx& [\eta_{11}^{(2)}, \eta_{12}^{(2)}, \ldots, \eta_{1M+1}^{(2)}, \eta_{21}^{(2)}, \ldots, \eta_{N+1+N_l\, M+1}^{(2)}]. \end{aligned}$$

The semi discrete approximations of the PML equations are

$$\begin{aligned} I_x \otimes I_y \otimes \partial_t^2 v + \Sigma \otimes I_y \otimes \partial_t v = D_{xx} \otimes I_y \otimes v + I_x \otimes D_{yy} \otimes v \qquad (39) \\ +\Sigma D_x \otimes I_y \otimes \zeta^{(1)} + \Sigma \otimes I_y \otimes (\alpha v + \zeta^{(2)}) + \Sigma' \otimes I_y \otimes \zeta^{(1)} \\ +I_x \otimes I_y \otimes f(v, \partial_t v)) + \text{SAT}_x + \text{SAT}_y, \end{aligned}$$

$$I_x \otimes I_y \otimes \partial_t \zeta^{(1)} = -D_x \otimes I_y \otimes v + (\alpha I_x + \Sigma) \otimes I_y \otimes \zeta^{(1)}, \tag{40}$$

$$I_x \otimes I_y \otimes \partial_t \zeta^{(2)} = I_x \otimes D_{yy} \otimes v - I_x \otimes I_y \otimes (\alpha^2 v + \alpha \zeta^{(2)}). \tag{41}$$

where $\otimes$ denotes the Kronecker product, defined for a $p \times q$ matrix A and a $r \times s$ matrix B as

$$A \otimes B = \begin{bmatrix} a_{11}B & \cdots & a_{1q}B \\ \vdots & & \vdots \\ a_{p1}B & \cdots & a_{pq}B \end{bmatrix}.$$

I_x and I_y are $N+1+N_l \times N+1+N_l$ and $M+1 \times M+1$ identity matrices, $\Sigma = \text{diag}(\sigma(x_i))$, $\Sigma' = \text{diag}(\partial_x \sigma(x_i))$, D_{xx} and D_{yy} are second derivative SBP operators of size $N+1+N_l \times N+1+N_l$ and $M+1 \times M+1$. D_x is a first derivative SBP operator, defined in [20], of size $N+1+N_l \times N+1+N_l$.

The boundary conditions are imposed by the penalty terms

$$\text{SAT}_x = (\tau_l H^{-1} E_0 (a_l I + b_l S) + \tau_r H^{-1} E_{N+1N_l} (a_r I + b_r S)) \otimes I_y \otimes v,$$
$$\text{SAT}_y = I_x \otimes (\tau_d H^{-1} E_0 (a_d I + b_d S) + \tau_u H^{-1} E_M (a_u I + b_u S)) \otimes v,$$

where subscripts l, r, d, u denotes *left, right, down* and *up*. Note that no boundary conditions should be imposed on $\eta^{(1)}$. For the discrete approximation this simply means that one sided difference (i.e. the SBP operators without the SAT term) are used to approximate $\partial_x \eta^{(1)}$.

For all of our experiments we will use the 8th order SBP operators with full norm (see appendix D.3 in Mattsson and Nordström, [20]). For homogenous Dirichlet boundary conditions we choose $\tau = -\gamma/h$ with $\gamma = 4.50$, for homogenous Neumann or mixed boundary conditions we choose the τ's according to equation (26).

In order to integrate the discrete solution in time by the 8th order 12 stage Runge-Kutta method (denoted NEW8(6) in [25]) proposed in [25] we introduce $q = \partial_t u$ and rewrite (39) as a first order system in time.

Remark 10. To estimate the maximum timestep we computed the spectral radius, ρ_{SR}, of the matrix on the right hand side of (39) with homogenous Dirichlet boundary conditions and without the damping terms and the nonlinear term. For this particular setup we found it to be $\rho_{SR} = 37.7$. Combining this with the imaginary stability limit 2.91 of the Runge-Kutta method the following condition on the time step the linear problem (assuming $h_x = h_y$)

$$dt \leq 2.91/\sqrt{\rho_{SR}}.$$

For the nonlinear and damped problem we started from the linear limit of the time-step and determined empirically a smaller time-step that produced stable solutions. Typically the size of the timestep was not affected by the damping terms but had to be reduced (sometimes significantly) as the coefficients of the nonlinearities were increased.

6.2 Nonlinear Experiments

The results obtained with our nonlinear PML will be compared with results obtained using the standard damping layer suggested by Israeli and Orzag

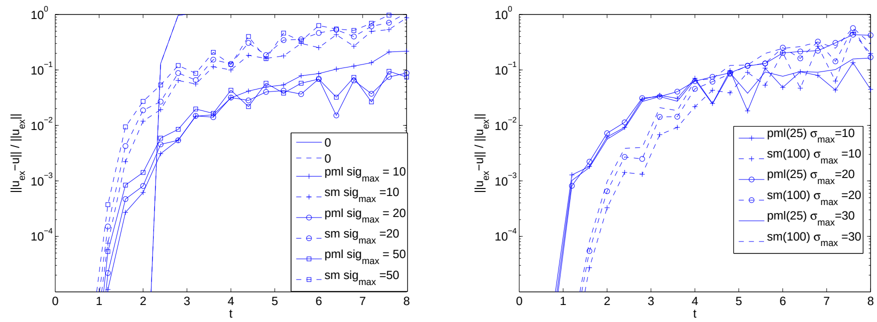

Fig. 4. Relative error for different times for a nonlinearity, $1.0u^3$. To the left the results for layers of width 0.5 are displayed, to the right results for a simple layer of width 1.0 and the PML of width 0.25.

[15], adopted to the nonlinear wave equation,

$$\partial_t^2 u - \nabla^2 u = -f(u, \partial_t u) + \sigma(x)\left(\partial_t u + \partial_x u\right). \tag{42}$$

The drawback of this layer is that it does not have the perfectly matched property. The advantage is that it does not require any auxiliary variables and thus is less memory consuming.

The simple layer is discretized in the same way as the PML (described in the previous section). In all nonlinear computations we use spatial step sizes $h_x = h_y = 1/50$. For simplicity we empircally chose a timstep that was stable for the most non-linear case below and use it for all the computations. We note that this result in an unnecessary small time step, which (as one reviewer pointed out) may lead to larger dispersion errors.

6.2.1 Experiment 1

In our first experiment we solve (1) with the nonlinearity (2) with $c_1 \neq 0$ and all other c_j and d_j set to zero. In this experiment we let $L_x = L_y = 1$ and consider the following initial data

$$u(0, x, y) = 10 \exp(-((x - 0.5)^2 + (y - 0.5)^2)/0.1^2),$$
$$\partial_t u(0, x, y) = 0.$$

We use homogenous Dirichlet boundary conditions on all boundaries and compare the solutions with a reference solution obtained by computing the solution in a wave guide in $(x, y) \in [0, 10] \times [0, 1]$.

In Figure 4 results for the simple layer and our PML, for $c_1 = 1.0$, are presented. In the left subfigure we compare results for layers of width 0.5. Since we store 4 variables $(u, q, \eta^{(1)}, \eta^{(2)})$ in the PML layer but only 2 in the simple layer (u, q) the latter requires only half of the memory compared to the PML.

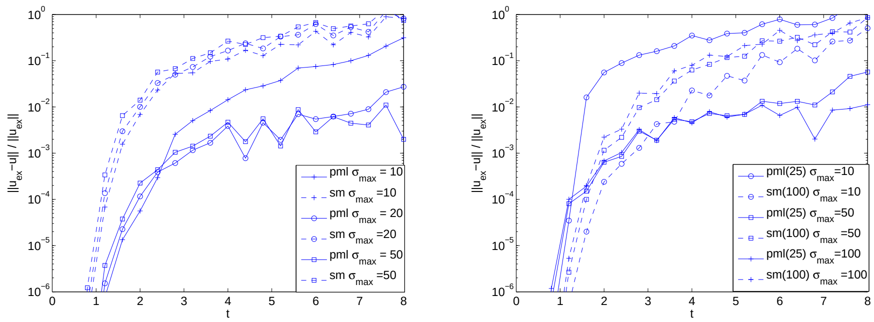

Fig. 5. Relative error for different times for a weaker nonlinearity, $0.1u^3$. To the left the results for layers of width 0.5 are displayed, to the right results for a simple layer of width 1.0 and a PML of width 0.25.

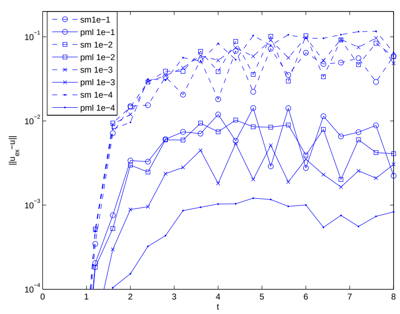

Fig. 6. Comparison between of errors for the simple layer and the PML (denoted sm and pml in the legend) for different strengths for performance a $d_1 \partial_t u^3$ nonlinearity. The strength ranges from 0.1-0.0001.

When both layers have the same width it is clear that the PML outperforms the simple layer but at some additional cost in memory. In the right subfigure we compare the results obtained from a simple layer of width 1.0 and the new layer of width 0.25. The results are roughly equal but it should be noted that now the new layer only requires half of the memory used by the simple layer. Thus we conclude that the PML is more efficient.

In Figure 5 we see the results for a weaker nonlinearity, $c_1 = 0.1$. To the left, results for both layers having the width 0.5, are displayed. To the right the simple layer have width 1.0 and the new layer have width 0.25. With this weaker nonlinearity the PML outperforms the simple layer also for the 1 / 0.25 setup, as can be seen in the right subfigure.

6.2.2 Experiment 2

The initial data and boundary conditions in this experiment are the same as in the previous experiment, but here we take d_1 non-zero. In Figure 6 a comparison between absolute errors for the simple layer and PML, for different

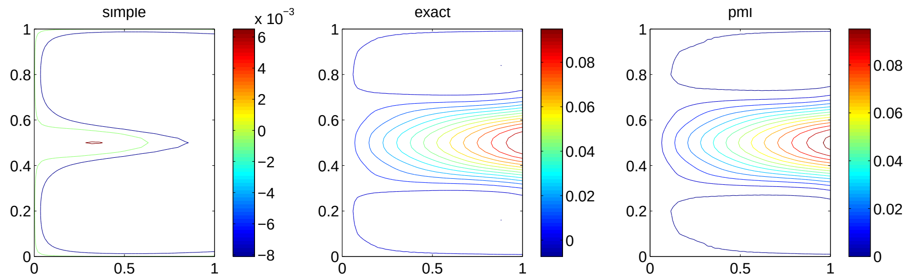

(a) Strength $d_1 = 0.1$

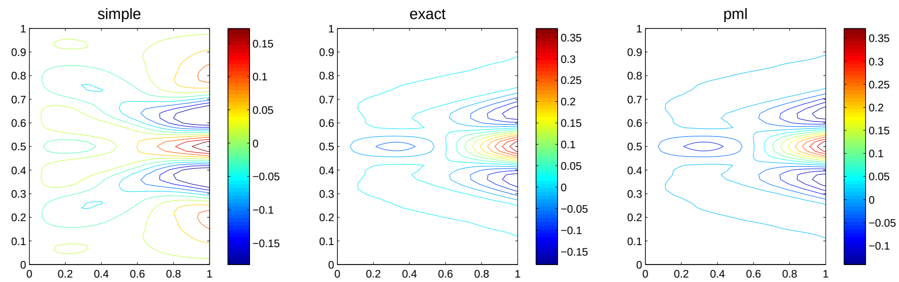

(b) Strength $d_1 = 0.001$

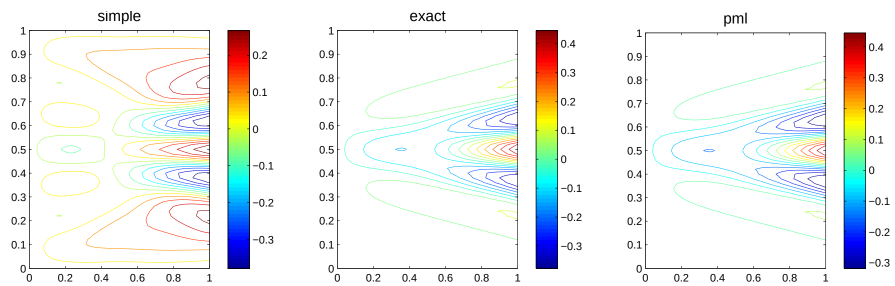

(c) Strength $d_1 = 0.00001$

Fig. 7. The figure displays the solution (at $t = 8$) obtained using the simple layer (to the left), the exact solution (in the middle) and he solution obtained using the PML (to the right). The uppermost pictures correspond to the strength $d_1 = 0.1$ the middle to the strength $d_1 = 0.001$ and the lower to the strength $d_1 = 0.00001$.

strengths ($d_1 = 0.1 - 0.0001$) of the nonlinearity, are plotted. Both the simple and the PML are of width 0.5. It is clear that the PML perform better and better as the strength of the nonlinearity decreases while the performance of the simple layer remains constant.

In Figure 7 the exact, the PML and the simple layer solutions at time $t = 8$ are plotted. The solution obtained using the PML agrees very well with the exact solution while the agreement of the solutions obtained using the simple layer and the exact solution is considerably worse.

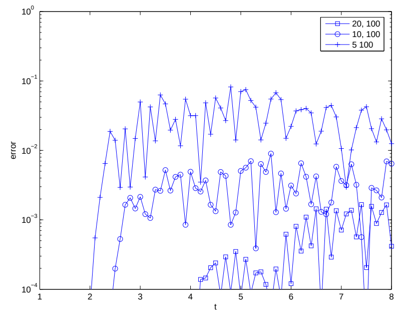

Fig. 8. Errors measured in the norm (43). The results should be compared with the results in Figure 5 in [6].

6.3 *Comparison with High Order Non-reflecting Boundary Conditions for a Linear Dispersive Problem*

Our last experiment is taken from [6] and is performed in order to compare the PMLs performance for a linear dispersive problem. In this example we solve (1) with $c_0 = 1$ and take all other c_j and d_j to zero. We solve the problem in the wave guide $(x, y) \in [0, 3] \times [0, 3]$. As in [6] we take the initial data to be

$$u(0,x,y) = \begin{cases} 2x \cos \frac{4\pi y}{3} & x < 0.5 \\ 2(1-x) \cos \frac{4\pi y}{3} & 0.5 < x < 1 \\ 0 & x > 1 \end{cases}, \quad \partial_t u(0,x,y) = 0.$$

We use homogenous Dirichlet boundary conditions on the boundary $x = 0$ and homogenous Neumann boundary conditions on $y = 0, 3$. The solutions are compared to a reference solution obtained by computing the solution in a wave guide in $(x, y) \in [0, 9] \times [0, 3]$. As in [6] we choose the space discretization to be $h_x = h_y = 3/60$. Also, we use the norm of the error

$$E(t) = \sqrt{\sum_{j=1}^{61} (u(t,3,y_j) - u_{ex}(t,3,y_j))^2}, \tag{43}$$

along $x = 3$. The results are plotted in Figure 8. Comparing with Figure 5 in [6] we see that the results for the PML with 5 points in the layer are comparable with the results with 5 auxiliary variables (J=5) in [6]. We note (from Figure 8) that the error can be decreased further by simply widening the layer.

7 Summary

We have derived a PML-like damping layer for a nonlinear dispersive wave equation of second order. In the layer only two auxiliary variables are needed. In the linear case the layer is perfectly matched, but in the nonlinear case it is not. In the linear case well-posedness is also established.

We show that the layer is stable in the following sense. In the linear, constant coefficient case stability is proven by analyzing a related algebraic problem. We also prove various energy estimates which can be used as a starting point for establishing stability of more general cases, such as with variable damping coefficients and nonlinear dispersive terms. In particular, we are able to show estimates for a special type of nonlinearity. In the numerical computations performed no instabilities were observed, even in cases where our theoretical estimates were not valid.

Two sets of numerical experiments were performed in order to compare the effectiveness of our layer with other techniques. In the first set we compared with a simpler layer by Israeli and Orzag. Their layer is not perfectly matched even in the linear case, but it requires no auxiliary variables. In the second set of computations we solved a linear dispersive problem. We compared the performance of our layer with results by Givoli, Neta and Patlatschenko, obtained using high order non-reflecting boundary conditions. In both cases our layer performed better or at least as well.

In the computations we use an eighth order summation-by-parts discretization in space and implement the boundary conditions using a penalty procedure. We present new stability results for this discretization applied to the second order wave equation in the case with Dirichlet boundary conditions.

A Appendix

A.1

Before proving Theorem 1 we first prove the following lemma.

Lemma 11. *Consider the Cauchy problem for the system (10-12) with σ and*

α constant. All solutions satisfy

$$\begin{aligned}
&\frac{1}{2}\frac{d}{dt}\Big(E(t) + 2\left(\partial_x\partial_t u + \alpha\partial_x u, \sigma(\partial_t\eta^{(1)} + \alpha\eta^{(1)})\right)\\
&\qquad + \sigma(\sigma+2\alpha)\|\partial_t\eta^{(1)} + \alpha\eta^{(1)}\|^2 + \|\sigma\partial_t\eta^{(1)}\|^2 + \|\sigma\alpha\eta^{(1)}\|^2\Big)\\
&\quad = -2\sigma\|\partial_t\eta^{(1)} + \alpha\eta^{(1)}\|^2 - 2\alpha\|\sigma\partial_t\eta^{(1)}\|^2 - \mathcal{F},
\end{aligned}$$

where

$$\mathcal{F} = \Big(\partial_t^2 u + (\sigma+\alpha)\partial_t u, f(u,\partial_t u)_t + (\sigma+\alpha) f(u,\partial_t u)\Big). \tag{A.1}$$

Proof of Lemma 11. We will only prove the result for real solutions. The extension to complex functions is straightforward. By integration by parts, and using (10) we obtain

$$\begin{aligned}
\frac{d}{dt}E = &\Big(\partial_t^2 u + (\sigma+\alpha)\partial_t u,\\
&\quad \partial_t^3 u + \sigma\partial_t u - \partial_x^2\partial_t u - \partial_y^2\partial_t u\alpha(\partial_t^2 u - \partial_x^2 u - \partial_y^2 u) - \sigma\partial_y^2 u\Big) +\\
&- (\sigma\partial_x\partial_t u, \partial_x\partial_t u + \alpha\partial_x u) =\\
= &\Big(\partial_t^2 u + (\sigma+\alpha)\partial_t u, \sigma(\partial_t\partial_x\eta^{(1)} + \alpha\partial_x\eta^{(1)})\Big) - (\sigma\partial_x\partial_t u, \partial_x\partial_t u + \alpha\partial_x u)\\
&- \Big(\partial_t^2 u + (\sigma+\alpha)\partial_t u, f(u,\partial_t u)_t + (\sigma+\alpha) f(u,\partial_t u)\Big) =: I_1 + I_2 + I_3.
\end{aligned}$$

By integration by parts we have

$$\begin{aligned}
I_1 + I_2 = &-\sigma\left(\partial_t^2\partial_x u + \alpha\partial_x\partial_t u, \partial_t\eta^{(1)} + \alpha\eta^{(1)}\right)\\
&- \sigma\left(\partial_x\partial_t u, \sigma(\partial_t\eta^{(1)} + \alpha\eta^{(1)}) + \partial_x\partial_t u + \alpha\partial_x u\right)\\
= &-\sigma\frac{d}{dt}\left(\partial_x\partial_t u + \alpha\partial_x u, \partial_t\eta^{(1)} + \alpha\eta^{(1)}\right)\\
&+ \sigma\left(\partial_x\partial_t u + \alpha\partial_x u, \partial_t^2\eta^{(1)} + \alpha\partial_t\eta^{(1)}\right)\\
&- \sigma\left(\partial_x\partial_t u, \sigma(\partial_t\eta^{(1)} + \alpha\eta^{(1)}) + \partial_x\partial_t u + \alpha\partial_x u\right).
\end{aligned}$$

By using (11) to express $\partial_x\partial_t u$ and $\partial_x u$ in the last two inner products above in terms of $\eta^{(1)}$, the lemma follows. □

Proof of Theorem 1. Note that

$$\begin{aligned}
&\|\partial_x\partial_t u + \alpha\partial_x u\|^2 + 2\left(\partial_x\partial_t u + \alpha\partial_x u, \sigma(\partial_t\eta^{(1)} + \alpha\eta^{(1)})\right)\\
&\quad + \sigma(\sigma+2\alpha)\|\partial_t\eta^{(1)} + \alpha\eta^{(1)}\|^2\\
&\quad = \|\partial_x\partial_t u + \alpha\partial_x u + \sigma(\partial_t\eta^{(1)} + \alpha\eta^{(1)})\|2 + 2\sigma\alpha\|\partial_t\eta^{(1)} + \alpha\eta^{(1)}\|^2.
\end{aligned}$$

Thus the theorem follows from Lemma 11 by integrating over time. □

To prove Theorem 4 we simply integrate the equality in the following lemma over time.

Lemma 12. *Consider the Cauchy problem for the system (10-12) with (20), σ constant and $\alpha = 0$. All solutions satisfy*

$$\begin{aligned}\frac{d}{dt}(\|\partial_t^2 u\|^2 + \|\partial_t\partial_y u\|^2 + \|\partial_x\partial_t u\|^2 + 2\left(\partial_x\partial_t u, \sigma\partial_t\eta^{(1)}\right) + \|\sigma\partial_t\eta^{(1)}\|^2 + \\ +\sigma\|\partial_y\eta^{(1)}\|^2 + \|\sigma\eta^{(2)}\|^2 + \|\sigma\partial_y u\|^2 + c\|\sigma u\|^2 + c\|\partial_t u\|^2 + c\|\sigma\eta^{(1)}\|^2) = \\ -\sigma\left(\|\partial_t^2\eta^{(1)}\|^2 + \|\partial_t\eta^{(2)} - \partial_t^2 u\|^2 + \|\partial_t\partial_y\eta^{(1)}\|^2 + c\|\partial_t\eta^{(1)}\|^2\right)\end{aligned}$$

Proof. Let

$$2I = \|\partial_t^2 u\|^2 + \|\partial_t\partial_y u\|^2 + \|\partial_x\partial_t u\|^2.$$

After integration by parts, and by using (10) we obtain

$$\begin{aligned}\frac{d}{dt}I &= \left(\partial_t^2 u, \partial_t^3 u - \partial_x^2\partial_t u - \partial_y^2\partial_t u\right) = \\ &= \left(\partial_t^2 u, -\sigma\partial_t^2 u + \sigma\partial_x\partial_t\eta^{(1)} + \sigma\partial_t\eta^{(2)} - \partial_t f(u, \partial_t u)\right).\end{aligned}$$

Introduce

$$\begin{aligned}I_1 := \left(\partial_t^2 u, \sigma\partial_x\partial_t\eta^{(1)}\right),\ I_2 := \left(\partial_t^2 u, \sigma\partial_t\eta^{(2)} - \sigma\partial_t^2 u\right), \\ I_3 := -\left(\partial_t^2 u, \partial_t f(u, \partial_t u)\right).\end{aligned}$$

By integrating by parts and using (11) we obtain

$$\begin{aligned}I_1 &= -\sigma\frac{d}{dt}\left(\partial_x\partial_t u, \partial_t\eta^{(1)}\right) - \sigma\left(\partial_t^2\eta^{(1)} + \sigma\partial_t\eta^{(1)}, \partial_t^2\eta^{(1)}\right) = \\ &= -\sigma\frac{d}{dt}\left(\partial_x\partial_t u, \partial_t\eta^{(1)}\right) - \sigma\|\partial_t^2\eta^{(1)}\|^2 - \frac{1}{2}\frac{d}{dt}\|\sigma\partial_t\eta^{(1)}\|^2.\end{aligned}$$

Adding and subtracting $\partial_t\eta^{(2)}$ to the first factor in I_2 results in

$$I_2 = -\sigma\|\partial_t\eta^{(2)} - \partial_t^2 u\|^2 + \sigma\left(\partial_t\eta^{(2)}, \eta_t^{(2)} - \partial_t^2 u\right).$$

From (12) and (10) it follows that

$$I_2 = -\sigma\|\partial_t\eta^{(2)} - \partial_t^2 u\|^2 + \sigma\left(\partial_t\eta^{(2)}, \sigma\partial_t u - \partial_x^2 u - \sigma\partial_x\eta^{(1)} - \sigma\eta^{(2)}\right).$$

To get a useful expression we use (12) and (11), yielding

$$
\begin{aligned}
I_2' &= \sigma\left(\partial_t\eta^{(2)}, \sigma\partial_t u - \partial_x^2 u - \sigma\partial_x\eta^{(1)}\right) \\
&= \sigma\left(\partial_y^2 u - f(u,\partial_t u), \sigma\partial_t u + \partial_x\partial_t\eta^{(1)}\right) = -\frac{\sigma^2}{2}\frac{d}{dt}\|\partial_y u\|^2 \\
&- \sigma^2\left(f(u,\partial_t),\partial_t u\right) + \sigma\left(\partial_x\partial_y u, \partial_t\partial_y\eta^{(1)}\right) + \sigma\left(\partial_x f(u,\partial_t u), \partial_t\eta^{(1)}\right).
\end{aligned}
$$

Using (20), and (11) to eliminate u from the last two terms yields

$$
\begin{aligned}
I_2' = &-\frac{1}{2}\frac{d}{dt}\left(\|\sigma\partial_y u\|^2 + c\|\sigma u\|^2 + \sigma\|\partial_y\eta^{(1)}\|^2 + c\|\sigma\eta^{(1)}\|^2\right) \\
&- \sigma\|\partial_t\partial_y\eta^{(1)}\|^2 - c\sigma\|\partial_t\eta^{(1)}\|^2.
\end{aligned}
$$

It follows that

$$
I_2 = -\sigma\|\partial_t\eta^{(2)} - \partial_t^2 u\|^2 + I_2' - \frac{1}{2}\frac{d}{dt}\|\sigma\eta^{(2)}\|^2.
$$

The term I_3 is easily estimated using (20),

$$
I_3 = -\frac{c}{2}\frac{d}{dt}\|\partial_t u\|^2.
$$

Lemma 12 follows. □

References

[1] S. Abarbanel, S. Stanescu, and M. Y. D. Hussaini. Unsplit Variables Perfectly Matched Layers for the Shallow Water Equations with Coriolis Forces. *Computational Geosciences*, 7(4):275–294, 2003.

[2] D. Appelö. *Absorbing Layers and Non-Reflecting Boundary Conditions for Wave Propagation Problems.* PhD thesis, Kungliga Tekniska Högskolan, October 2005.

[3] D. Appelö, T. Hagstrom, and G. Kreiss. Perfectly Matched Layers for Hyperbolic Systems: General Formulation and Energy Estimates. *SIAM J. Appl. Math.*, 67:1–23, 2006.

[4] E. Bécache and P. Joly. On the analysis of Bérenger's perfectly matched layers for Maxwell's equations. *Math. Mod. Numer. Anal.*, 36(1):87–119, 2002.

[5] M. H. Carpenter, D. Gottlieb, and S. Abarbanel. The stability of numerical boundary treatments for compact high-order finite-difference schemes. *Journal of Computational Physics*, 108:272–295, 1993.

[6] Givoli, Neta, and Patlashenko. Finite element analysis of time-dependent semi-infinite wave-guides with high-order boundary treatment. *Int. J. Numer. Meth. Engng.*, 58(13):1955–1983, 2003.

[7] D. Givoli and B. Neta. High-order non-reflecting boundary scheme for time-dependent waves. *J. Comput. Phys*, 186:24–46, 2003.

[8] T. Hagstrom. New results on absorbing layers and radiation boundary conditions. In M. Ainsworth, P. Davies, D. Duncan, P. Martin, and B. Rynne, editors, *Lecture Notes in Computational Science and Engineering*, volume 31, chapter T. Hagstrom Topics in Computational Wave Propagation, pages 1–42. Springer-Verlag, New York, 2003.

[9] T. Hagstrom. Perfectly matched layers for hyperbolic systems with applications to the linearized Euler equations. In Cohen et. al, editor, *Mathmatical and Numerical Aspects of Wave Propagation, Proceedings Waves2003*, pages 125–129. Springer Verlag, 2003.

[10] T. Hagstrom and D. Appelö. Automatic Symmetrization and Energy Estimates Using Local Operators for Partial Differential Equations. *Communications in Partial Differential Equations*, 2006. To appear.

[11] T. Hagstrom and T. Warburton. High-order local radiation boundary conditions: Corner compatibility conditions and extensions to first order systems. *Wave Motion*, 39:327–338, 2004.

[12] R.L. Higdon. Absorbing boundary conditions for difference approximations to the multidimensional wave equation. *Math. Comp.*, 47:437–459, 1986.

[13] L. Hörmander. *Lectures on nonlinear hyperbolic differential equations*, volume 26 of *Mathematiques & Applications*. Springer-Verlag, 1997.

[14] F. Q. Hu. On the construction of PML absorbing boundary condition for the non-linear Euler equations. Technical Report 2006-0798, AIAA, 2006.

[15] M. Israeli and S.A. Orzag. Approximation of radiation boundary conditions. *J. Comput. Phys.*, 41:115–135, 1981.

[16] S. Kichenassamy. Nonlinear wave equations. In *Monographs and Textbooks in Pure and Applied Mathematics*, volume 194 of *38-5A194*, page 296. Marcel Dekker, 1995.

[17] H-O. Kreiss and J. Lorenz. *Initial-Boundary Value Problems and the Navier-Stokes Equations*. Academic Press Inc., 1989.

[18] S. Lee, B. Janko, I. Derenyi, and A. L. Barabasi. Reducing vortex density in superconductors using the 'ratchet effect. *Nature London*, 400:337, 1999.

[19] J. Maddox. Making models of muscle contraction. *Nature*, 365:203, 1993.

[20] K. Mattsson and J. Nordström. Summation by parts operators for finite difference approximations of second derivatives. *J. Comput. Phys.*, 2004.

[21] L. Morales-Molina, F.G. Mertens, and A. Sanchez. Ratchet behavior in nonlinear Klein-Gordon systems with pointlike inhomogeneities. *Physical Review E*, 72, 2005.

[22] L. Morales-Molina, N.R. Quintero, A. Snchez, and F.G. Mertens. Soliton ratchets in homogeneous nonlinear klein-gordon systems. *Chaos*, 16:013117, 2006.

[23] C. Sogge. *Lectures on nonlinear wave equations*. Cambridge University Press, 1993.

[24] J. Szeftel. A nonlinear approach to absorbing boundary conditions for the semilinear wave equation. *Math. Comp.*, 75:565–594, 2006.

[25] Ch. Tsitouras and S. N. Papakostas. Cheap error estimation for Runge-Kutta methods. *SIAM J. Sci. Comput.*, 20:2067–2088, 1999.